

Charge Transfer and Disorder in Double Perovskites

Nieves Menéndez,[†] Mar García-Hernández,^{*,‡} Diana Sánchez,[‡] Jesús D. Tornero,[†] José L. Martínez,[‡] and José A. Alonso[‡]

Departamento de Química Física Aplicada, Universidad Autónoma de Madrid, and Instituto de Ciencia de Materiales de Madrid, CSIC, Cantoblanco, E-28049 Madrid, Spain

Received April 30, 2004. Revised Manuscript Received June 24, 2004

The effect of disorder due to anti sites on the charge-transfer processes in the double perovskite $\text{Sr}_2\text{FeMoO}_6$ has been assessed at the microscopic level, using ^{57}Fe Mössbauer spectroscopy. We have followed over a very broad temperature range (from 673 to 4.2 K) the spectral response of three polycrystalline samples only differing in the levels of anti-site disorder of the B sublattice. Our measurements reveal an intricate charge-transfer pattern across T_C that is connected to the levels of disorder present in each sample. It is found that the magnetic transition triggers a charge-transfer process between the ordered and anti-site disordered regions for moderate levels of disorder, while this process is completely disabled when disorder becomes dominant. The observed behavior is correlated to the macroscopic properties of the system.

Introduction

The current search for materials potentially useful for applications in the field of spintronics has brought about a renewed interest in the study of the double perovskites A_2FeMoO_6 , where A is an alkaline-earth element. This interest is prompted in the case of $\text{Sr}_2\text{FeMoO}_6$ (SFMO) by the findings of Kobayashi et al.,¹ Tomioka et al.,² and Sarma et al.,³ according to which the polarization of the conduction electron is almost complete even at room temperature. The band structure exhibits a gap for the majority spin band where the $3d^5$ up-spin electrons localize around the high-spin ion Fe^{3+} , while the ungapped minority band is partially occupied by the $4d^1$ spin electrons of the Mo^{5+} ions. From Mössbauer spectroscopy (MS), evidence has been given to support the degenerate nature of the fundamental state as the result of the existing equilibrium $\text{Fe}^{3+} + \text{Mo}^{5+} \leftrightarrow \text{Fe}^{2+} + \text{Mo}^{6+}$ in which the itinerant down-spin electron is shared by both types of atoms⁴ rendering a +2.5 effective valence to Fe ions.

The system was initially proposed^{1,2} to be ferrimagnetic with important antiferromagnetic (AF) interactions between the neighboring Fe and Mo ions. According to this model, the system would exhibit a large saturation moment of $4 \mu_B$. Also, the predominant ferrimagnetism would lead to an effective ferromagnetic (FM) interaction between Fe ions separated by a Mo, and would explain roughly the calculated phase diagram.⁵

However, the microscopic magnetic and electronic structure of this material has been revealed to be controversial. Neutron diffraction data show a wide spread of values for the magnetic moment attached to Mo ions, ranging from $0 \mu_B$ ⁶ to $1 \mu_B$.⁷ Ray et al.⁸ from X-ray absorption spectroscopy (XAS) give an upper limit for the absolute value of the magnetic moment for Mo around $0.25 \mu_B$. These authors propose that the delocalized down-spin electron of the Mo sites is transferred via hybridization to the neighboring Fe (45%) and O (30%), allowing only 25% of the minority spin to remain in the surroundings of Mo sites. The localized high-spin Fe^{3+} ion ($S = 5/2$) would couple antiferromagnetically with the delocalized down-spin density, lowering the Fe ion spin to form an $S = 2$ state. The most recent experimental results seem, however, to definitely confirm a ferrimagnetic ground state for $\text{Sr}_2\text{FeMoO}_6$ ^{9,10} with a magnetic moment of $-0.35 \mu_B$ on the Mo ion.

The ongoing controversy is further magnified by the almost unavoidable presence of a certain amount of disorder in the structure of real samples. It is well-known that perovskites $\text{A}_2\text{B}'\text{B}''\text{O}_6$ with a charge difference between B' and B'' greater than 2 present various degrees of disorder in the alternating positions of the B' and B'' cations.¹¹ In $\text{Sr}_2\text{FeMoO}_6$ this means that a certain fraction (denoted as x , with $0 < x < 0.5$) of Mo

* To whom correspondence should be addressed. Fax: +34 913720623. E-mail: marmar@icmm.csic.es.

[†] Universidad Autónoma de Madrid.

[‡] CSIC.

(1) Kobayashi, K. I.; Kimura, T.; Sawada, H.; Terakura, K.; Tokura, Y. *Nature* **1998**, *395*, 677.

(2) Tomioka, Y.; Okuda, T.; Kumai, R.; Kobayashi, K. I.; Tokura, Y. *Phys. Rev. B* **2000**, *61*, 422.

(3) Sarma, D. D.; Mahadevan, P.; Saha-Dasgupta, T.; Ray, S.; Kumar, A. *Phys. Rev. Lett.* **2000**, *85*, 2549.

(4) Linden, J.; Yamamoto, T.; Karppinen, M.; Yamauchi, H.; Pietari, T. *Appl. Phys. Lett.* **2000**, *76*, 2925.

(5) Chattopadhyay, A.; Millis, A. J. *Phys. Rev. B* **2001**, *64*, 024424.

(6) García-Landa, B.; Ritter, C.; Ibarra, M. R.; Blasco, J.; Algarabel, P. A.; Mahendiran, R.; García, J. *Solid State Commun.* **1999**, *110*, 435.

(7) Chamaissen, O.; Kruk, R.; Dabrowski, B.; Brown, D. E.; Xiong, X.; Kolesnik, S.; Jorgensen, J. D.; Kimball, C. W. *Phys. Rev. B* **2000**, *62*, 14197.

(8) Ray, S.; Kumar, A.; Sarma, D. D.; Cimino, R.; Turchini, S.; Zennaro, S.; Zerma, N. *Phys. Rev. Lett.* **2001**, *87*, 97204. Sarma, D. D. *Curr. Opin. Solid State Mater. Sci.* **2001**, *5*, 261.

(9) Tovar, M.; Causa, M. T.; Butera, A.; Navarro, J.; Martínez, B.; Fontcuberta, J.; Passegi, M. C. G. *Phys. Rev. B* **2002**, *66*, 24409.

(10) Besse, M.; Cros, V.; Barthelemy, A.; Jaffres, H.; Vogel, J.; Petroff, F.; Mirone, A.; Tagilaferrri, A.; Bencok, P.; Decorse, P.; Berthet, P.; Rogalev, A.; Fert, A. *Europhys. Lett.* **2002**, *60*, 608.

(11) Woodward, P.; Hoffmann, R.-D.; Sleight, a. W. *J. Mater. Res.* **1994**, *9*, 2118.

sites are occupied by Fe and vice versa. From now on, we refer to this sort of disorder as anti-site disorder (ASD). The presence of these defects changes significantly the magnetic picture described above. Indeed, the first consequence is the presence of AF interactions between consecutive (B' and B'') Fe, as initially conjectured by Ogale et al.¹² and confirmed by our neutron diffraction (ND) experiments.¹³ These AF correlations are responsible for the observed¹⁴ decrease of the saturated magnetization in the disordered system, since the spins of the Fe ions at Mo sites have opposite orientations to the spins of the Fe sublattice. Recently, it has also been proposed that the Curie temperature T_C of SFMO should increase slightly¹⁵ with the level of disorder, although the saturation magnetization is reduced when compared with that of the fully ordered compound. The postulated small increase of T_C would also point out the tendency toward FM coupling of the Fe at the ordered positions (B') enhanced by the strong AF interactions between consecutive Fe ions, as already mentioned above.

Notice that ASD can be easily visualized as a generator of regions for which the alternation of Fe and Mo atoms in the structure gives way to islands consisting of clusters of oxygen octahedra whose centers are all occupied by Fe atoms or all by Mo atoms. We will refer to these regions as ASD patches. ASD has been shown to be a major issue in the understanding of the low-field magnetoresistance properties of these materials.¹⁶ However, the effects of ASD on the microscopic magnetic and electronic structure of the system are scarce and still a matter of debate. The valence state of Fe in SFMO has already been studied previously, but ASD effects have been only partially addressed.^{4,7,14,17–19} Linden et al.⁴ from MS, in addition to the most abundant component corresponding to an effective valence of +2.5 for Fe, reported a less abundant spectral component related to ASD and compatible with a high-spin Fe³⁺ state. Chamaissen et al.⁷ interpret this latter component of the Mössbauer spectra in terms of the existence of Mo vacancies, adding some particularities to the local environment of the near neighbor Fe atom. No allowances for ASD effects are made in this case. Greneche et al.,¹⁸ also from MS, conclude that point anti-site defects predominate over anti-phase boundaries, and 3d^{5.2} is postulated as the electronic configuration for Fe ion in the ordered compound.¹⁹

The purpose of this paper is to systematically assess the role of ASD in determining the electronic configura-

tion of Fe in the structure and to relate the observed changes to the evolution of the magnetic degrees of freedom. For such a purpose we have performed a series of Mössbauer experiments. This spectroscopy is a local probe technique where three parameters are of paramount importance in the parametric description of the spectra: the isomer shift (δ), the hyperfine magnetic field (B_{hf}), and the quadrupole splitting (ΔQ). The isomer shift provides information on the electron densities and, hence, on the valence state and coordination number of the probe atom in the sample under study. A single-line spectrum is expected when local magnetic fields or nonuniform electric fields do not exist in the loci occupied by the probe nucleus, while a local magnetic field splits the spectrum into six lines. Therefore, the amount of magnetic splitting renders valuable information on the magnetic state of the sample at a very local level, allowing discrimination between ordered and disordered environments around ⁵⁷Fe. To disentangle the role of ASD in determining the valence state of the system at a local level, we have worked with three samples, labeled *ordered*, *semiordered*, and *disordered*, whose ASD levels strongly differ. These have been previously characterized by neutron and/or X-ray diffraction and magnetometry.¹³ Due to the complexity of the magnetic interactions present in the system and its intricate evolution across T_C , we have followed the spectral response over a very broad temperature range (from 673 to 4.2 K), probing the system at small temperature steps to ensure a consistent assignment of the various contributions to the experimental spectra. This strategy marks a clear difference from previously reported MS studies. In particular, we focus on the evolution of the charge-transfer processes through the Curie temperature, $T_C \approx 415$ K, and the relevance of the disorder-induced charge effects is then discussed within the context of the low-field magnetoresistance properties of this material.¹⁶

Experimental Section

Powders of SFMO with different degrees of ASD ordering were prepared by soft chemistry procedures. Stoichiometric amounts of analytical grade Sr(NO₃)₂, FeC₂O₄·H₂O, and (NH₄)₆Mo₇O₂₄·4H₂O were dissolved in citric acid. The citrate + nitrate solutions were slowly evaporated, leading to an organic resin containing a homogeneous distribution of the involved cations. This resin was first dried at 120 °C and then slowly decomposed at temperatures up to 600 °C. All the organic materials and nitrates were eliminated in a subsequent treatment at 800 °C in air for 2 h. This treatment gave rise to a highly reactive precursor material. The *disordered* sample was obtained after a thermal treatment at 850 °C for 2 h in a H₂/N₂ (15%/85%) reducing flow. The *semiordered* sample was prepared from a batch of the previously synthesized disordered one by heating it for 12 h at 1050 °C in a H₂/N₂ (5%/95%) flow. The *ordered* sample was also synthesized from the usual precursors but subsequently was fired at 1100 °C for 12 h in a H₂/Ar (1%/99%) reducing flow, to favor the B-cation ordering.

Structural characterization of the samples was made by X-ray diffraction. The degree of ordering for both samples was established by Rietveld analysis of the X-ray diffraction patterns within the tetragonal space group (*I4/m*), according to the NPD results at room temperature. The *ordered* and *semiordered* samples show superstructure peaks, (e.g., (011) and (013)) arising from the Fe/Mo alternating order in the double perovskite structure, while only a small diffuse intensity remains at these angles for the *disordered* sample. The

(12) Ogale, A. S.; Ogale, S. B.; Ramesh, R.; Venkatesan, T. *Appl. Phys. Lett.* **1999**, *75*, 537.

(13) Sánchez, D.; Alonso, J. A.; García-Hernández, M.; Martínez-Lope, J. M.; Martínez, J. L.; Mellergard, A. *Phys. Rev. B* **2002**, *65*, 104426.

(14) Balcells, LL.; Navarro, J.; Bibes, M.; Roig, A.; Martínez, B.; Fontcuberta, J. *Appl. Phys. Lett.* **2001**, *78*, 781.

(15) Alonso, J. L.; Fernández, L. A.; Guinea, F.; Lesmes, F.; Martín-Mayor, V. *Phys. Rev. B* **2003**, *67*, 214423.

(16) García-Hernández, M.; Martínez, J. L.; Martínez-Lope, M. J.; Casais, M. T.; Alonso, J. A. *Phys. Rev. Lett.* **2001**, *86*, 2443.

(17) Sarma, D. D.; Sampathkumaran, E. V.; Ray, S.; Nagarajan, R.; Majumdar, S.; Kumar, A.; Nalini, G.; Guru Row: T. N. *Solid State Commun.* **2000**, *114*, 465.

(18) Greneche, J. M.; Venkatesan, M.; Suryanarayanan, R.; Coey, J. M. D. *Phys. Rev. B* **2001**, *63*, 174403.

(19) Douvalis, A. P.; Venkatesan, M.; Coey, J. M. D.; Grafoute, M.; Greneche, J. M.; Suryanarayanan, R. *J. Phys.: Condens. Matter* **2002**, *14*, 12611.

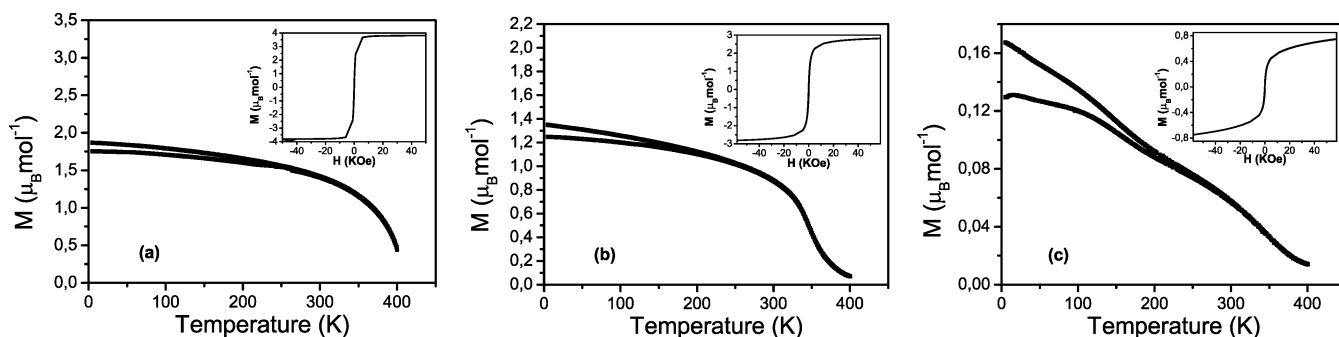


Figure 1. Zero-field-cooled magnetization vs temperature measured at 1000 Oe: (a) *ordered* sample, (b) *semiordered* sample, (c) *disordered* sample. The insets show the corresponding hysteresis cycles at 5 K.

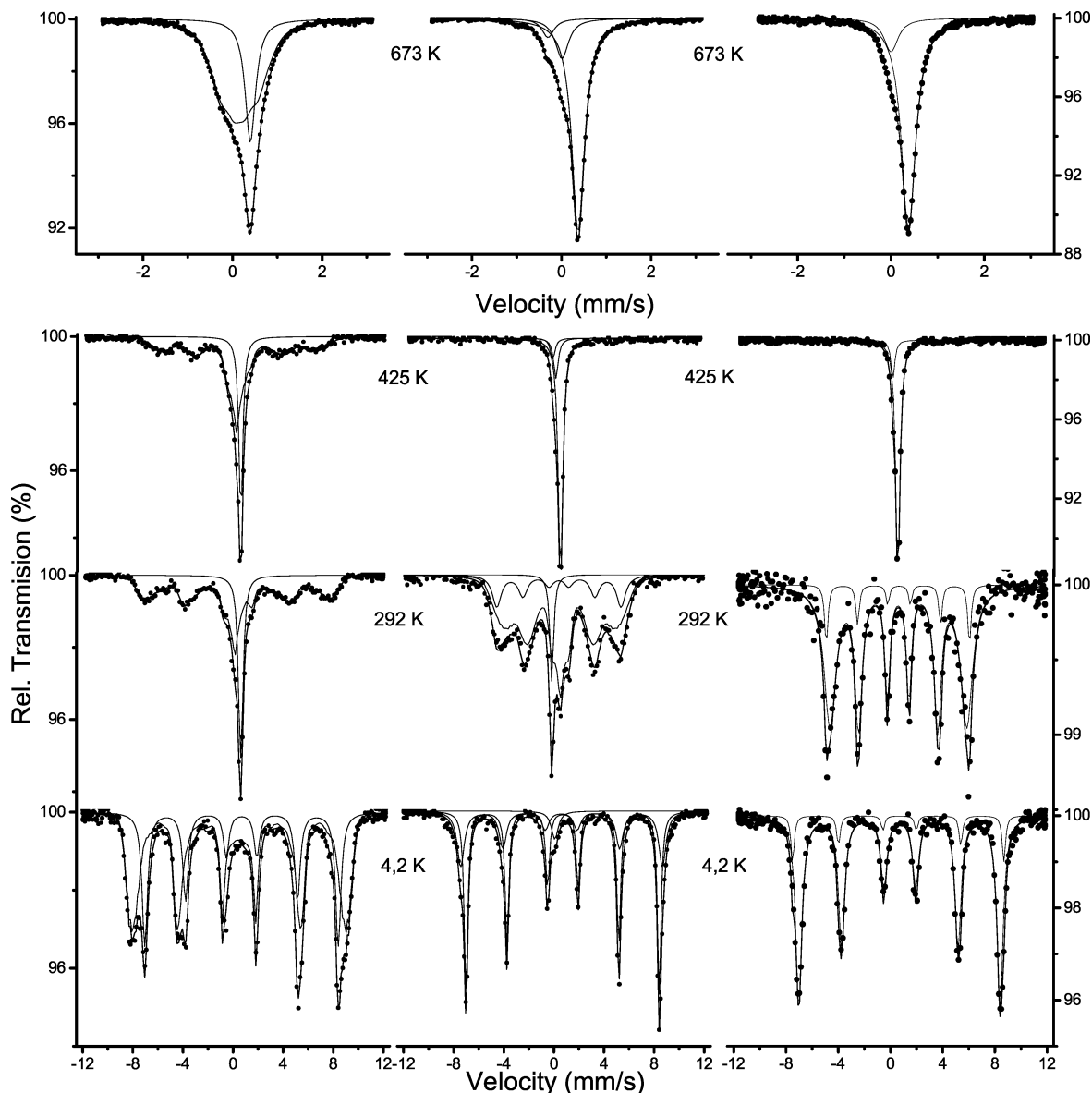


Figure 2. Representative Mössbauer spectra at different temperatures along with the different components described in the text: (left) *disordered* sample, (middle) *semiordered* sample, (right) *ordered* sample.

degree of ordering, defined as $100(1 - 2x)$, was estimated to be $\sim 93\%$, $\sim 68\%$, and $\sim 18\%$ for the *ordered*, *semiordered*, and *disordered* samples, respectively. From neutron diffraction experiments, we conclude that samples are oxygen-stoichiometric within standard deviation.

As shown in Figure 1, from SQUID magnetometry measurements under an applied field of 1000 Oe, large differences can be seen in the magnetization of the samples. For the *ordered* sample the magnetization shows a neat transition at T_C from

a paramagnetic state at high temperature to a ferromagnetic/ferrimagnetic (FM) one at low temperature. The saturation moment at 5 K is $3.8 \mu_B/\text{fu}$. A similar behavior is found for the *semiordered* sample, although the saturated moment decreases now to $2.8 \mu_B/\text{fu}$. By contrast, the *disordered* sample shows a smoother FM transition that at 5 K renders a saturation moment of $0.8 \mu_B/\text{fu}$. This strong suppression of the FM properties is related to the ASD. It has been shown^{12,14} that the magnetization, M_S , of a particular sample, derived under

Table 1. Mössbauer Hyperfine Parameters Corresponding to Figure 2

Sr ₂ FeMoO ₆	T(K)	δ^a (mm/s)	B _{hf} (T)	%
ordered	673	0.374(2)		88
		0.001(4)		12
	425	0.533(2)		89
		0.15(1)		11
	292	0.591(8)	32.4(1)	89
		0.58(1)	34.0(1)	11
4.2	0.707(1)	47.8(1)	89	
	0.640(7)	50.1(1)	11	
semiordered	673	0.371(2)		78
		0.009(4)		15
	425	-0.300(9)		7
		0.536(1)		78
	292	0.169(4)		13
		-0.142(6)		9
	0.590(1)	25.0(3)	75	
		0.48(3)	30.7(2)	18
	4.2	-0.092(7)		7
		0.704(1)	47.8(1)	76
0.599(3)	50.5(1)	17		
	-0.07(1)		7	
disordered	673	0.398(2)		26
		0.153(6)	3.4(4)	74
	425	0.578(2)		25
		0.367(8)	35.8(3)	75
	292	0.63(3)		25
		0.31(8)	37.5(4)	75
4.2	0.771(3)	47.8(1)	24	
	0.49(2)	50.5(2)	76	

^a Relative to α -Fe.

the assumption of AF coupling between the Fe and Mo sublattices and magnetic moments of 5 and 1 μ_B for Fe and Mo cations, respectively, is given by $M_S = (4 - 8x) \mu_B/\text{fu}$, where x has been defined previously as the fraction of Fe atoms replaced by Mo atoms in the perfect structure. Introducing in this equation the disorder fraction extracted from the X-ray diffraction measurements, we recover saturation moments of 3.75, 2.72, and 0.72 μ_B/fu for the *ordered*, *semiordered*, and *disordered* samples, respectively, in good agreement with the measured values.

The Mössbauer spectra have been recorded in sinusoidal mode using a conventional spectrometer with a ⁵⁷Co/Rh source. To avoid saturation effects and to optimize the signal-to-noise ratio, the sample thickness was 10 mg of ^{nat}Fe/cm². The analysis of the spectra was made by a nonlinear fit using the NORMOS program,²⁰ and the energy calibration was made with α -Fe (6 μm) foil. An NB sample holder was used for high-temperature measurements, while another one with Be windows was used in the low-temperature range. Figure 2 shows representative spectra at different temperatures, and Table 1 gives the most relevant Mössbauer hyperfine parameters.

Results

A. "Ordered" Sample. As is apparent from Figure 2, at either the low-temperature or high-temperature ends, the spectra are the result of the convolution of two well-defined subspectra, while in the medium-temperature range they exhibit a larger complexity.

At temperatures above T_C , in the paramagnetic regime, two independent single lines of different intensities are observed with a half-width at half-maximum (Γ) around 0.36(1) mm/s and a χ^2 value of 1.14. Although the value of Γ is slightly high, we think that there are not substantial distortions associated with the oxygen octahedron, in agreement with previous ND data that render above T_C a cubic structure ($Fm\bar{3}m$) for the

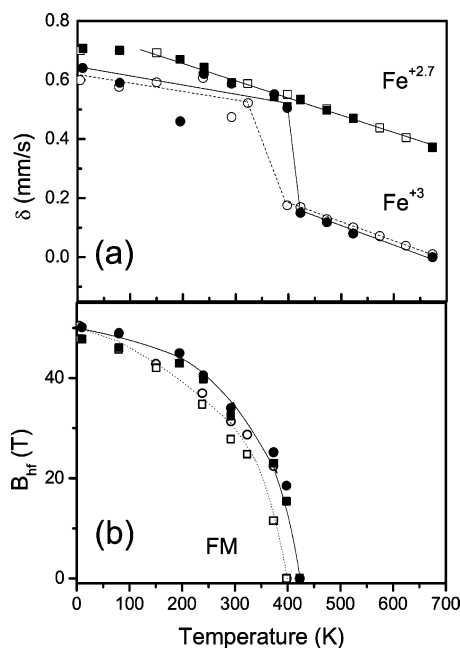


Figure 3. (a) Evolution of the Mössbauer isomer shift with temperature for the *ordered* sample (solid symbols) and for the *semiordered* sample (open symbols). Squares refer to Fe^{2.7+} and circles to Fe³⁺. (b) Temperature dependence of the hyperfine field. Symbols are as in (a). Lines are only a guideline for the eye.

ordered double perovskite.¹³ The most abundant component (89% of the resonant area) shows an isomer shift (δ) of 0.374(2) mm/s at 673 K (see Figure 3), in agreement with the reported values. The assignment of this component to a particular species is still a matter of debate.^{4,18} Greneche et al. assigned it to a +2.7 valence for Fe, taking as a reference value for the isomer shift of Fe²⁺ that corresponding to Sr₂FeWO₆. In contrast, Linden et al. related this component to a +2.5 species, with reference to the value of 0.78 mm/s for Fe²⁺ in the very low end of the generally accepted range. Clearly, the valence state of Fe in this system must rest between +2 and +3, but there is no unambiguous evidence to precisely favor one assignment over the other since, as already mentioned, there is a wide spread of values in the literature on the magnetic moment located at the Mo ions. We attach to Greneche's assignment, Fe^{2.7+}, since the adopted Fe²⁺ reference correlates finely, at least on structural grounds, with our double perovskite system.

Also at this temperature, 673 K, there is a single line showing a significantly smaller isomer shift, $\delta = 0.001(4)$ mm/s, that we associated with the second component (with 12% of the resonant area). This δ value is in accordance with the expected value for an Fe³⁺ in an undistorted octahedron. The observed relative intensity of this component leads us to assign it to Fe occupying the Mo sites in the structure. Since the ASD defects in the *ordered* samples correspond basically to point defects (tiny ASD patches), no large distortions of the local symmetry are expected, which is consistent with the cubic structure for an ordered sample above T_C .¹³ This is in contrast to what has been proposed in the literature, where an important crystallographic distortion around Fe³⁺ is postulated due to the existence of Mo vacancies⁷ or, alternatively, to unspherical electric fields generated by ASD.¹⁸ In both cases a quadrupolar

(20) Brand, R. A. *Nucl. Instrum. Methods Phys. Res., B* **1987**, *28*, 398.

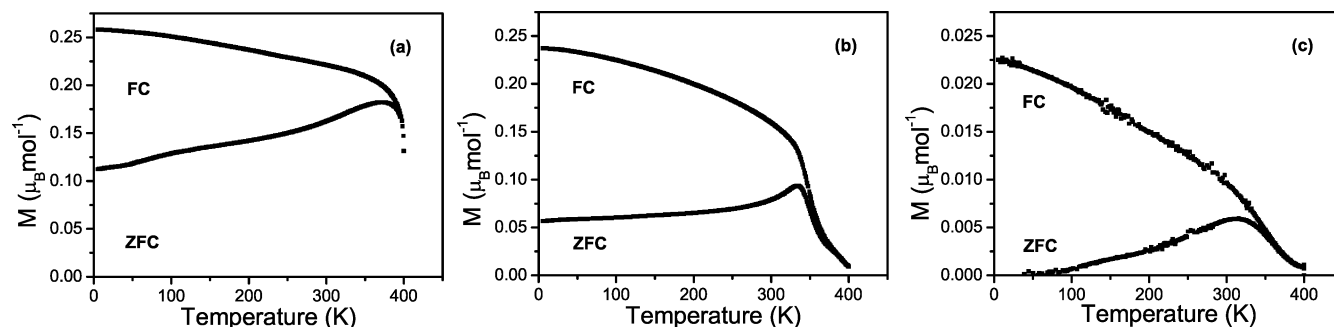


Figure 4. Zero-field-cooled and field-cooled magnetization vs temperature measured at 50 Oe: (a) *ordered* sample, (b) *semiordered* sample, (c) *disordered* sample.

doublet is then used in the analysis of the Fe^{3+} contribution. From our Mössbauer spectra we do not find evidence of such a distorted environment.

At low temperatures (4.2 K), the spectrum is consistent with two sextets. With the only restriction of keeping the intensity ratio 3:2:1 for both sextets and equal Γ values within each sextet, the principal components show relative intensities of 89% and 11%, in agreement with the high-temperature results. It is also worth mentioning that the magnetic transition occurs together with a structural transition from a cubic ($Fm\bar{3}m$) to a tetragonal ($I4/m$) structure.^{7,13}

In the intermediate region, between the magnetic transition (approximately at 400 K) and the low-temperature end (4.2 K), the experimental area is well accounted for by two magnetic contributions. One sextet corresponds to the Fe^{3+} subspectrum. The other magnetic component, a broad sextet corresponding to $\text{Fe}^{2.7+}$, narrows as the temperature decreases and the average internal field increases. The resulting $\text{Fe}^{2.7+}:\text{Fe}^{3+}$ intensity ratios obtained from the fits are in agreement with that of the low- and high-temperature limits.

The temperature evolution of the isomer shifts corresponding to both components are given in Figure 3a. As expected, see Figure 3b, the magnetic hyperfine fields, B_{hf} , for $\text{Fe}^{2.7+}$ and Fe^{3+} are very similar but slightly larger for the latter.

B. “Disordered” Sample. For the *disordered* sample the situation completely differs. The existence of AF correlations up to 700 K in the Fe-rich ASD patches¹³ means that even at 675 K a small magnetic contribution is still apparent in the Mössbauer spectrum. As in the case of the *ordered* sample, the experimental spectra are well fitted with a two-component model corresponding to species $\text{Fe}^{2.7+}$ and Fe^{3+} .

The high-temperature spectra, up to 673 K, were interpreted as the sum of two terms: a single line (25% of the resonant area) with an isomer shift that coincides with the $\text{Fe}^{2.7+}$ component of the *ordered* sample and that, therefore, was assigned to the ordered clusters within the disordered matrix and a second and most abundant contribution, corresponding to Fe^{3+} , that is a distribution of hyperfine magnetic fields with approximately 75% of the resonant area, matching the levels of ASD present in the sample. The statistical quality of the fit is revealed by a low χ^2 value of 1.12. For the latter component (Fe^{3+}), the same value of $\delta = 0.153(6)$ mm/s at 673 K is derived if we consider a quadrupole splitting distribution. However, a magnetic field distribution is preferred since the existence of an antiferromagnetic

coupling at temperatures as high as 700 K has been well established from magnetization and ND data.¹³

On lowering the temperature to near 200 K, the experimental intensities are described as the sum of a distribution of hyperfine magnetic fields due to the AF correlations for the Fe^{3+} species, plus the $\text{Fe}^{2.7+}$ component that remains unsplit. Below 200 K, down to 4.2 K, the magnetic splitting of the latter is also observed. This is fully consistent with the phenomenology observed in the macroscopic magnetization in the intermediate temperature range. Figure 4 shows the zero-field-cooled–field-cooled (ZFC–FC) magnetization curves measured at $H = 50$ Oe, a condition more similar to that of the Mössbauer experiment at zero applied field. The behavior exhibited by the system upon cooling in the absence of a magnetic field is compatible with the phenomenology exhibited by a blocking process of an assembly of superparamagnetic particles with a distribution of blocking temperatures around $T_C = 310$ K. It should now be recalled that the Mössbauer experiments measure the local blocking of the spins without determining the various alignments and that the decay process of the Mössbauer effect has an intrinsic lifetime of 10^{-7} s. This means that if a spin cluster is blocked on a time scale longer than 10^{-7} s, the hyperfine splitting will appear, regardless of the orientation of the blocked spin. This will not be the case if the blocking time is shorter than the typical time scale of the Mössbauer experiment, and consequently, only an unsplit component will be apparent. The fact that the subspectrum corresponding to the FM ordered patches within the AF disordered matrix splits at $T = 200$ K marks the crossing at this temperature of the two relevant time scales, that of the relaxation of the magnetization between equivalent easy orientations of the FM ordered clusters and that of the Mössbauer experiment.²¹ It is expected that the strong irreversibility associated with the blocking process of the magnetic clusters would disappear with application of a magnetic field of a few kilooersteds, as the anisotropy field of the particles is surpassed and the clusters are saturated. Indeed, a strong reduction of the irreversibility is observed as the applied field is increased up to 1000 Oe, but a small anomaly (a kink) can be seen around 200 K (see Figure 1). This anomaly could be reminiscent of the blocking process of the superparamagnetic clusters. However, alternative scenarios such as the existence of a cluster-glass-like behavior, compat-

(21) Hoy, G. R. In *Mössbauer Spectroscopy Applied to Inorganic Chemistry*; Long G. J., Ed.; Plenum Press: New York, 1984; Vol. 1.

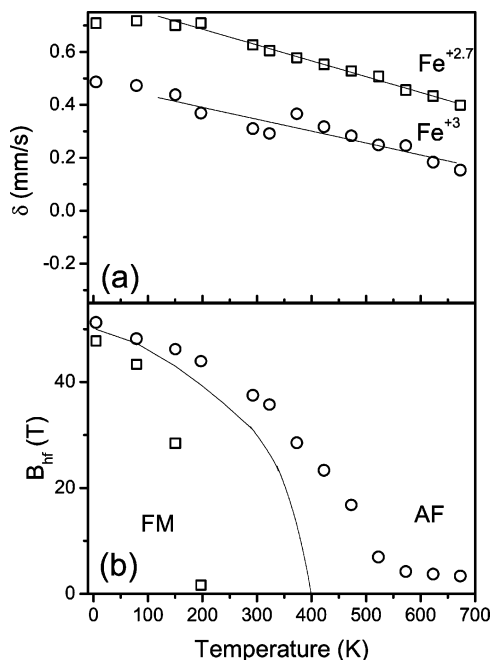


Figure 5. (a) Evolution of the Mössbauer isomer shift with temperature for the *disordered* sample. Squares refer to $\text{Fe}^{2.7+}$ and circles to Fe^{3+} . (b) Temperature dependence of the hyperfine magnetic field. Symbols are as in (a). Lines are only a guideline for the eye.

ible also with the dramatic drop observed in the ZFC curve at 50 Oe for the *disordered* sample, cannot be ruled out. The experimental discrimination between superparamagnetic behavior and the freezing of a cluster-spin glass is not trivial and is out of the scope of the present paper. The relevant information that can be extracted from the ZFC–FC curves is the absence of long-range FM correlations and the existence of an important amount of frustration in ordered patches as expected from the strong AF long-range correlations in the disordered matrix. It should also be mentioned that irreversibilities and, therefore, blocking processes are attached to the presence of ASD. This is further confirmed by the smaller irreversibilities and the flatter temperature dependence of the ZFC curve observed in the ordered samples (see Figure 4).

The magnetic field distribution can be ascribed to the presence of Fe^{3+} in different environments. Probably anti-site defects in the *ordered* sample are well represented by single substitutions of Fe ions occupying Mo sites (that is, Fe ions surrounded by six other Fe atoms). However, in the *disordered* sample, as the ASD concentration is much higher, it is possible to find Fe ions surrounded by different combinations of atoms (5Mo/1Fe, 4Mo/2Fe, ..., 1Mo/5Fe, and 6Fe), giving rise to slightly different values of δ , ΔQ , and B_{hf} and, consequently, a broader quadrupole or magnetic field distribution. This, certainly, can also be the origin of the increase of the average isomer shift for the nominally Fe^{3+} in the *disordered* sample by comparison with its value in the *ordered* one. However, we do not observe any displacement for the $\text{Fe}^{2.7+}$ component (see Figures 3a and 5a).

Regarding the hyperfine field shown in Figure 5b, the slow decrease of B_{hf} for Fe^{3+} , which even at $T = 673$ K is 3.4 T, is quite remarkable, while in the *ordered* sample it drops sharply to zero at $T = 415$ K (Figure

3b). The behavior of the $\text{Fe}^{2.7+}$ component also shows a fast drop to zero at around 200 K, compatible with the macroscopic magnetic measurements. At first sight it seems puzzling that B_{hf} is the same for both samples, around 50 T, at low temperatures, while saturated moments lie so far apart, according to the magnetization measurements. This is, however, well understood in light of the magnetic model proposed for the disordered material. According to it, strong AF correlations prevail in the Fe-rich patches that do not contribute to the magnetization of the sample but generate local fields (either positive or negative) that are readily probed without distinction by MS. Indeed, the hyperfine values extrapolate to zero at a temperature close to that at which AF correlations set in within the ASD patches.¹³

C. “Semioordered” Sample. As an independent assessment of the soundness of the physical picture emerging from samples exhibiting unlike ASD levels, we have reproduced the experimental Mössbauer profiles of a third sample exhibiting an intermediate ordering of the B sublattice. To interpret the spectra consistently, it has been necessary to measure their evolution within a wide temperature range ($4.2 \text{ K} < T < 673 \text{ K}$).

The spectra are described basically as the sum of two components assigned to the species $\text{Fe}^{2.7+}$ and Fe^{3+} with relative intensities of 76% and 17%, respectively, in good agreement with the reported values for the ordered and disordered fractions in this sample.¹³ In the paramagnetic regime, a χ^2 value of 1.2 is obtained for the fit and a very small contribution to the spectral area is also required with an isomer shift close to that of Fe^{4+} . Similar contributions have been reported in the literature, and they have been assigned either to the presence of Fe^{4+} in the sample²² or to an experimental artifact stemming from the cryostat window.⁴ However, the chemistry of these materials, prepared in a strongly reducing atmosphere, seems to preclude the presence of Fe^{4+} , and the measurement of the empty container seems also to discard the presence of this species in any component of the experimental setup.

It is quite remarkable that even at temperatures as low as 150 K some zero-field contribution remains in the magnetic field distribution of $\text{Fe}^{2.7+}$, as also reported by Douvalis et al.¹⁹ This contribution, probably associated with Fe ions in highly frustrated regions (i.e., boundaries between ordered and ASD domains) points out the difficulties experienced by these spins to align below T_C .

The jump in the Fe^{3+} isomer shift as well as the drop to zero of B_{hf} occurs in this sample at temperatures slightly lower than that observed for the *ordered* sample, which is consistent with the lower measured T_C .

Discussion

From the Mössbauer spectroscopy results we can conclude that there exists a dominant component corresponding to a large matrix for each sample. This matrix coaches superparamagnetic clusters that result from the tiny size of the less abundant patches in both

(22) Sakuma, H.; Taniyama, T.; Kitamoto, Y.; Yamazaki, Y. *J. Appl. Phys.* **2003**, *93*, 2816.

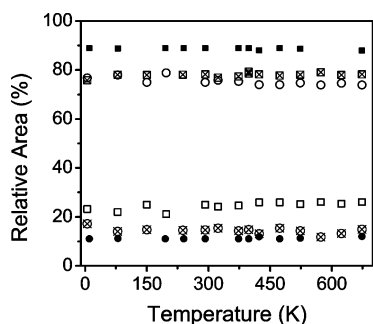


Figure 6. Relative proportion of $\text{Fe}^{2.7+}$ (squares) and Fe^{3+} (circles) from the Mössbauer areas. Solid symbols refer to the *ordered* sample, crossed symbols to the *semiordered* sample, and open symbols to the *disordered* sample.

samples. Line shape broadening is mainly observed for the dominant components, and these have been analyzed as a hyperfine magnetic field distribution in each sample.

In the *disordered* sample the matrix (most abundant component Fe^{3+}) is antiferromagnetic in the whole temperature range, since it orders above 770 K.¹³ Also for this sample the clusters (least abundant component $\text{Fe}^{2.7+}$) align FM well below T_C , at 200 K. This is consistent with the magnetic behavior expected for small clusters that experience difficulties in aligning FM since the surroundings are strongly AF.

In the *ordered* sample the matrix (most abundant component $\text{Fe}^{2.7+}$) is paramagnetic above $T_C \approx 415$ K and ferromagnetic below T_C . Here, the tiny clusters (least abundant species Fe^{3+}) remain disordered below $T_N \approx 770$ K, because of the paramagnetic environment surrounding these clusters. Below T_C , within the small cluster, FM correlations develop, due to the strong influence (direct exchange) of the ferromagnetic matrix (i.e., clusters behave as soft magnets inside the FM matrix).

In brief, our samples have been analyzed in terms of one superparamagnetic component (below T_N for the *disordered* and below T_C for the *semiordered* and *ordered* samples) plus another dominant component (FM in the *semiordered* and *ordered* samples and AF in the *disordered* one). Most remarkably, it is found that this model is the only one that provides the required physical constraint of keeping the anti-site disorder ratios constant for each sample within the entire explored temperature range (see Figure 6). The presence of anti-phase boundaries, recently reported in the literature,^{18,23} cannot be ruled out in these samples. However, the good agreement between the measured saturated magnetization and a modeling of the magnetization for a “random microdomain ASD”,¹⁸ using as input the ASD percentages measured by X-ray diffraction, leads us to think that the contribution from APB to disorder is probably small.

From the isomer shift results in Figures 3a and 5a, the following facts are apparent.

(1) The component $\text{Fe}^{2.7+}$ (associated with the ordered regions) shows the same isomer shifts in all samples, and the observed evolution with temperature is fully

explained in terms of a simple Debye–Waller model and the second-order Doppler shift.

(2) The component Fe^{3+} (associated with the ASD regions) displays large differences. The most striking feature for this component is the sharp change of the isomer shift observed around T_C for the *ordered* and *semiordered* samples in contrast to the smooth behavior displayed by the *disordered* one. This fact deserves some comment: our experimental Mössbauer data for the *ordered* and *semiordered* samples could also be analyzed in terms of the model proposed by Greneche et al.¹⁸ that assumes a tetragonal lattice for $\text{Sr}_2\text{FeMoO}_6$ not only below T_C but also above T_C . This modeling results in isomer shifts for the Fe^{3+} that do not display any jump at T_C . However, when we analyze the spectra in terms of these two quadrupole doublets, a change in the intensity ratios for the ordered and disordered portions is observed as the temperature varies. This behavior is not compatible with the well-established fact that anti-site disorder for a particular sample remains constant in the whole temperature range explored, and it is also in contradiction with the cubic lattice structure found above T_C for the ordered samples from our previous ND experiments.¹³ Thus, we have adopted the alternative analysis, using the cubic structure above T_C ,¹³ since this is the only model preserving the correct intensity ratios for the different components through the temperature range explored (Figure 6). Our model, which is also fully consistent with the magnetic picture, leads to the conclusion that there is a net charge transfer from the ordered matrix to the disordered patches when T_C is crossed from above, for any highly ordered sample. This is related to the size of ASD clusters that below T_C , when the ordered regions align FM, experience the appearance of weak (somehow frustrated) FM short-range correlations also in the ASD Fe-rich patches. As a consequence, the electronic transport through these low barriers is enabled, and therefore, a decrease of the valence of the Fe in the ASD patches from +3 to +2.7 occurs, as inferred from the evolution of the isomer shift in Figure 3a. In contrast, the smooth behavior of the Fe^{3+} isomer shift observed for the *disordered* sample can be explained considering that the charge-transfer processes from the Mo-rich to the Fe-rich regions are confined to the FM/AF boundaries, being completely impeded well inside the disordered region, since there is no Mo available. The charge-transfer processes across *disordered* regions in the *ordered* (or *semidisordered*) sample is directly related to the low-field magnetoresistive properties of these materials. The small ASD regions in the more ordered samples act as electron scatterers and disrupt a large number of hoppings, which effectively increases the resistivity of these samples. The triggering of electronic transport across the small disordered regions on lowering the temperature or, alternatively, upon application of a small magnetic field decreases the resistivity of the sample and explains the large low-field magnetoresistance reported in samples with moderate levels of ASD.¹⁶ This is not the case for the *disordered* sample for which the percolation threshold is not reached due to the massive levels of disorder present.

In summary, we have provided a microscopic correlation of the role of ASD in determining the electronic

(23) Linden, J.; Karppinen, M.; Shimada, T.; Yasukawa, Y.; Yamachi, H. *Phys. Rev. B* **2003**, *68*, 174415.

configuration of Fe in the structure and have related the observed changes to the evolution of the magnetic degrees of freedom.

Acknowledgment. We acknowledge financial support from the Spanish CICyT (Grants MAT2002/01329 and MAT2001/0539), DGSIC (Grant PB98/0120), and

the Comunidad Autonoma de Madrid (Grant CAM-07N/0008/2001). Preparation and X-ray characterization of the samples by M. J. Martinez-Lope and M. Retuerto are acknowledged. We are thankful to Prof. F. Guinea for critical reading of the manuscript and fruitful discussions.

CM049305T